Alexandria Engineering Journal (2021) 60, 5851–5859

Alexandria University

Alexandria Engineering Journal

www.elsevier.com/locate/aej
www.sciencedirect.com

Generalized formulation to estimate the Supercapacitor's R-C series impedance using fractional order model

Kajal Kothari *, **Ravneel Prasad, Utkal Mehta**

School of Engineering and Physics, The University of the South Pacific, Laucala Campus, Fiji

Received 23 February 2020; revised 29 September 2020; accepted 3 April 2021

KEYWORDS

Fractional-order models;
Supercapacitor;
Haar operational matrix of derivative;
Impedance model;
Caputo definition.

Abstract The main objective of this paper is to develop a new technique for the supercapacitor's parameter identification that can handle the issue of initial voltage. An effective approach is proposed using the fractional-order derivative for accurate identification of a well-known series Resistance-Capacitance (R-C) model. An expression is derived using the Caputo definition and the Haar wavelet operational matrix, which is sufficient for both charging and discharging phase data of supercapacitors. To extract impedance parameters, voltage stimulated step response is utilized and parameters are calculated despite random initial voltage stored in a supercapacitor. This operational matrix approach transforms complex fractional derivative terms into simple algebraic expressions and reduces the overall complexity. The proposed technique shows a very good agreement with experimental data that exhibit different initial voltages and different time-frames. Investigations and experiments with various supercapacitors clearly reveal the importance of the developed equation for a fractional R-C model.

1. Introduction

Supercapacitors (SCs) have become unanimously vital elements in the diverse fields for energy accumulation and storage applications. They exhibit outstanding and exceptional properties like high power density, improved reliability, long lifespan, and instantaneous power supply compared to conventional capacitors and batteries. These properties render it as a promising technology, and increase the growth in the consumption of SCs in various energy management systems and power quality regulators, like electric vehicles, hybrid electric vehicles, uninterruptible power supplies, solar array systems, wind turbine systems, renewable systems, AC line filtering, and so on [1,2]. Unlike normal batteries that are heavy and bulky, the SC can store the energy without any chemical reaction, and accumulate the energy electrostatically. Due to higher surface area and capacitance with thinner dielectrics, it exhibits ten times higher power density than a battery and

* Corresponding author.
E-mail addresses: s11151029@student.usp.ac.fj (K. Kothari), s11108164@student.usp.ac.fj (R. Prasad), utkal.mehta@usp.ac.fj (U. Mehta).

Peer review under responsibility of Faculty of Engineering, Alexandria University.

https://doi.org/10.1016/j.aej.2021.04.018

a hundred times the higher energy density than the conventional capacitor.

Though there are many benefits of employing SCs, efficient energy storage is only possible with the precise modeling of the component characteristics. It is desirable to model SCs with high precision for safe and reliable operations. To note that the precise model can also help to improve the maintenance of many critical applications. Various techniques have been illustrated so far in the literature to deal with the parameter extraction of the SC. Mostly, these techniques have characterized the standard calculus-based models and followed the international standard IEC 62391. It is found that the SC models, based on conventional transfer functions, are similar to normal electrolytic capacitors. However, it is reported that the conventional model is not sufficient to extract information precisely [3]. There is a possibility of progressively worse energy efficiency due to the distinct diffusion phenomena of SCs. Because of unfitting characterization, it may provide inefficient modeling advantages of SCs in various energy applications. Moreover, the SC's characteristics change significantly with variations in the initial condition, aging, charging/discharging profile, and voltage excitation [1,2]. Therefore, estimating a standard SC model is not an easy problem.

Various techniques have been illustrated for the parameter extraction of the SC with different types of models. The online parameter estimation technique for SC using recursive least square was illustrated in [4] and using weighting bat algorithm was depicted in [5]. Considering distribution of relaxation times, another modeling approach using a dynamic equivalent circuit was described in [6]. The above techniques are based on classical approach.

Nowadays, fractional-order modeling has shown an increasing consideration due to their excellent ability to match experimental data even with less number of parameters [7,8]. Fractional model for electrical circuits such as RLC circuit was derived using Mittag-Leffler function (MLF) in [9]. The review of supercapacitor modeling with respect to fractional order electrical characterization in [2] and mathematical ways in [10] presented for quick understanding the research topic. The series Resistance-Capacitance (R-C) fractional-order impedance model was applied most commonly and also studied in detail by Freeborn et al. [11] and further revisited in [12,13] with more analysis related to real-time embedded applications and issues. A new SC model that consists of two parallel fractional capacitors, and a fractional order element was developed and analyzed by Martynyuk and Ortigueira [14]. A flexible SC model was discussed in [15] that omits the requirement of impedance structure selection and automatically select the best suitable structure that accurately fit the experimental data. Zhang et al. [16] suggested a new model for SC and addressed the issue of state-of-charge estimation. Abro et al. [17] analyzed De-Levie's model using fractional calculus for SC applications. Another model of SC for electrical vehicle applications, was described in [18]. Recently, a modeling technique of SC with analytical formulation in terms of power, energy, and efficiency was illustrated in [3]. Various state-of-art materials for SC were reviewed and analyzed in [19] with performance metrics and real-time application related issues.

Though some of the presented works followed the fractional calculus approach for the modeling and characterization, they have considered zero initial conditions. Moreover, the different initial conditions can modify the parameter values for the same SC data. Some of the previously reported methods yield a very high equivalent series resistance (ESR), which contradicts the low ESR property of SCs as per data-sheet information. Say, for example, the technique described in [11], was developed using zero initial conditions, and even though a very good curve fitting with the actual data, this method produced a high ESR value. This method was then extended in [20] with non-zero initial conditions. However, both methods [11,20] were developed for constant input and it can not be applied to the other types of inputs. For this work, authors have noted the above issues for future investigation to estimate the R-C series SC impedance parameters. Motivated by the unavailability of a generalized formulation for the SC impedance modeling technique, the work is presented in this paper to estimate the SC parameters independent of initial conditions, time range behavior, and excitation constraint.

This paper deals with the non-integer (fractional) derivative for the time-domain equation using the Haar operational matrices. An effective approach pertaining to an operational matrix method is developed by using Caputo derivative and the Haar wavelet, considering the non-zero initial condition. Analytical expressions of the non-integer (fractional) derivatives are developed using the Haar operational matrix in the time-domain. The investigation was carried out experimentally to check the robustness against the aforementioned limitations. It has been noted that the initial voltage in SCs can change the real-time model behavior and thus fails to perform consistently. When the initial voltage is being ignored, the identified ESR can be significantly larger than the suggested value in datasheet by manufacturers (see for example: AVX branded SC datasheet [21] suggests a very small value utmost 1 Ω). Hence, the proposed technique is developed with consideration of initial conditions. Furthermore, the method simplifies the handling of fractional differentiation of themeasured data by converting derivative terms into an algebraic expression. A single expression of the output voltage is sufficient for both charging and discharging cycles. The proposed estimation scheme for SCs' impedance also significantly outperforms with the charging-discharging cycle together. The experimental observations are pointed out the practical use of this accurate identification scheme. The contribution and novelties are summarized below.

- An operational matrix approach has been opted using the Haar wavelet that resulted in the more generalized output expression to represent the charging and discharging profiles of SCs.
- The developed output expression is sufficient for both charging and discharging data.
- For different values of supercapacitors, the parameters have been identified and analyzed with zero and non-zero initial conditions.
- The approach works accurately with different initial voltages and time frame data.
- The proposed technique deals with real-time noisy data without denoising or pre-processing

2. Prerequisites

2.1. Selection of fractional derivatives

Even though the fractional derivatives are being applied to the various scientific domain, it is crucial to understand the key

value of each definition in application fields. The fractional calculus with the Riemann-Liouville (RL) and Caputo (CP) derivatives are studied most commonly and alternatively used in the literature for the linear system theory, modeling, and identification purposes. Let's define the RL derivative as below [7],

$$ {}_R\mathcal{D}^{\lambda}x(t) = \frac{1}{\Gamma(n-\lambda)}\left(\frac{d}{dt}\right)^n \int_a^t \frac{x(\tau)}{(t-\tau)^{\lambda+1-n}}d\tau, \tag{1}$$

where λ is a non-integer order $(n-1<\lambda<n, n\in N)$ and Γ denotes Euler's gamma function. The Laplace transform with non-zero initial condition can be characterized as,

$$ \mathcal{L}\left[{}_R\mathcal{D}^{\lambda}x(t)\right] = s^{\lambda}X(s) - \sum_{k=0}^{n-1} s^k \left[{}_R\mathcal{D}^{\lambda-k-1}x(t)\right]_{t=0}. \tag{2}$$

The renowned CP derivative can be characterized by [7],

$$ {}_C\mathcal{D}^{\lambda}x(t) = \frac{1}{\Gamma(n-\lambda)}\int_0^t \frac{x^{(n)}(\tau)}{(t-\tau)^{\lambda-n+1}}d\tau. \tag{3}$$

After s-domain representation with non-zero initial condition, it can be illustrated by

$$ \mathcal{L}\left[{}_C\mathcal{D}^{\lambda}x(t)\right] = s^{\lambda}X(s) - \sum_{k=0}^{n-1} s^{\lambda-k-1}x^k(0). \tag{4}$$

Here, we are going to emphasize "initial conditions" and in particular case, we cannot always consider zero initial conditions for the SCs. The state of charge plays a vital role and can not be ignored for modeling purposes. It is studied that the RL derivative may be inappropriate as its Laplace transform has no physical interpretation with the non-zero initial conditions [22]. On the contrary, the Laplace transform of the CP derivative has known physical interpretation, and it handles the initial conditions similar to classical integer-order derivatives [23]. However, the CP definition is limited to fractional-order $\lambda \geqslant 0$ which shows differentiation. Therefore, the study with the Haar wavelet operational matrix of fractional order derivative using CP definition forms the base for our investigation to identify SC's impedance parameters with the non-zero initial conditions. In fact, this investigation develops a more comprehensive operational matrix approach that can handle the initial conditions in the model equation.

2.2. Fractional derivative with Haar operational matrix

The orthogonal Haar wavelet functions are utilized in this work due to high precision, mathematical simplicity, noise immunity, and ease of implementation with other standard algorithms. Computationally, Haar wavelets are faster compared to other functions of the wavelet family and exhibit the advantage of noise immunity [24]. The Haar wavelets can be defined as [25]

$$ h_m(t) = h_1(2^i t - kT_f), \tag{5}$$

where T_f is the total time period, $m = 2^i + k$, whereby $i\,(i \geqslant 0)$ and $k\ (0 \leqslant k \leqslant 2^i)$ are integers,

$$ h_0(t) = 1 \text{ for } 0 \leqslant t < T_f \text{ and } h_1(t) = \begin{cases} 1 & 0 \leqslant t < \frac{T_f}{2}; \\ -1 & \frac{T_f}{2} \leqslant t < T_f; \\ 0 & \text{otherwise.} \end{cases}$$

Now, an arbitrary function $x(t) \in L^2[0, T_f]$ can be written in terms of Haar wavelets for the first M number of terms as

$$ x(t) = \sum_{i=0}^{M-1} x_i h_i(t) = X_M^T H_M(t), \tag{6}$$

where $X_M \triangleq = [x_0, x_1, \ldots, x_{M-1}]^T$ is the Haar coefficient vector and $H_M(t) \triangleq = [h_0(t), h_1(t), \ldots, h_{M-1}(t)]^T$ is the Haar function vector. If collocation points are considered at the interval of $t_i = (2i-1)T_f/2M, (i = 1, 2, .., M)$, the M-square Haar matrix $\Phi_{M\times M}$can be defined by,

$$ \Phi_{M\times M} \triangleq \left[H_M\left(\frac{1}{2M}T_f\right)\ H_M\left(\frac{3}{2M}T_f\right)\ldots H_M\left(\frac{2M-1}{2M}T_f\right)\right]. \tag{7}$$

It is important here to use the merit of the Haar operational matrix in order to simplify the fractional-order derivatives (FOD). The Haar wavelet operational matrix of FOD can be obtained by using the operational matrix of FOD of the block pulse functions which is given by

$$ D^{\lambda}_{M\times M} = \left[F^{\lambda}_{M\times M}\right]^{-1}, \tag{8}$$

where M-square matrix $F^{\lambda}_{M\times M}$ is the operational matrix of fractional-order integration for block pulse functions, and written as

$$ F^{\lambda}_{M\times M} = \left(\frac{T_f}{M}\right)^{\lambda}\frac{1}{\Gamma(\lambda+2)}\begin{pmatrix} f_1 & f_2 & f_3 & \cdots & f_M \\ 0 & f_1 & f_2 & \cdots & f_{M-1} \\ \vdots & \ddots & f_1 & \cdots & f_{M-2} \\ \vdots & & \ddots & \ddots & \vdots \\ 0 & \cdots & \cdots & 0 & f_1 \end{pmatrix}_{(M\times M)}, \tag{9}$$

where $f_1 = 1, f_q = q^{\lambda+1} - 2(q-1)^{\lambda+1} + (q-2)^{\lambda+1}$ and $q = 2,3,\ldots,M$.

Now, the FOD of Haar wavelets can be obtained by its multiplication with the M-square matrix $B^{\lambda}_{M\times M}$. The algebraic expression of FOD of the Haar wavelet is written as

$$ \left(\mathcal{D}^{\lambda}\mathcal{H}_{\mathcal{M}}\right)(t) \approx B^{\lambda}_{M\times M}H_M(t), \tag{10}$$

where $B^{\lambda}_{M\times M}$ is called the Haar wavelet operational matrix of FOD, which is computed as

$$ B^{\lambda}_{M\times M} = \Phi_{M\times M}D^{\lambda}_{M\times M}\Phi^{-1}_{M\times M}. \tag{11}$$

In this way, the operational matrix approach transforms fractional differentiation problem into simple matrix multiplication.

3. Supercapacitor impedance model

In literature, various models have been reported to represent the SC based on its dynamic behavior. In this work, the elementary series R-C model is studied and analyzed due to its structural simplicity, and resemblance with the exact dynamic behavior of the actual SC. However, the proposed operational matrix method can be developed or extended to any other type of model or even a flexible SC model as discussed in [15]. It is shown in [11] that SCs follow closely non-integer (fractional) behavior and have fractional impedance composed of a series resistor (R_s) and fractional-order capacitor (C_{λ}). The total

Fig. 1 Fractional series R-C model of supercapacitors.

equivalent impedance of the R-C series SC model can be characterized as

$$Z(s) = R_s + \frac{1}{C_\lambda s^\lambda}, \tag{12}$$

where C_λ is the pseudo-capacitance with $0 \leqslant \lambda \leqslant 1$ order. Most common traditional capacitors are a small subset of a generalized form (12) when $\lambda = 1$. Fig. 1 shows the presented structure of fractional series R-C model.

3.1. Problem formulation

As illustrated in [11], the charging and discharging expressions for the SC impedance model are as below.

$$v_{o_{charge}}(t) = \left[V_{CC}\frac{t^\lambda}{C_\lambda(R+R_s)}E_{\lambda,\,\lambda+1}\left(\frac{-t^\lambda}{C_\lambda(R+R_s)}\right)\right] + \left[V_{CC}\frac{R_s}{(R+R_s)}E_{\lambda,\,1}\left(\frac{-t^\lambda}{C_\lambda(R+R_s)}\right)\right] \tag{13}$$

$$v_{o_{discharge}}(t) = v(0)\frac{R}{R+R_s}E_{\lambda,1}\left(\frac{-t^\lambda}{C_\lambda(R+R_s)}\right), \tag{14}$$

where E denotes MLF and V_{CC} is the magnitude of a step function. The following observations and limitations of these expressions are found:

- Expressions can fit the charging and discharging characteristics individually.
- The charging and discharging equations are explicitly dependent on time.
- Possibly the estimated model parameters are related to the time-frame of the data.
- It makes the estimation procedure more complex when the measured data is continuous for charging-discharging cycles.
- The charging expression was developed considering the zero initial voltage in SC.
- Static with only step input type.

Considering the fact that impedance parameters from output voltage vary with not only initial voltage or input's amplitude but also time range. It is vital to prove the parameters calculated from these expressions are independent of the initial state-of-charge and time-range. This warrants researchers for further investigation on how to estimate more accurate and reliable parameters for SC model.

4. Proposed parameter identification technique

The prime work is to stress on the identification of impedance parameters for SCs, considering initial conditions. The fractional R-C series SC model can give a response from the step input as [11]

$$V_o(s) = \frac{V_{in}(s)\frac{1}{C_\lambda(R+R_s)} + V_{in}(s)\,s^\lambda\frac{R_s}{(R+R_s)} + v(0)\,s^{\lambda-1}\frac{R}{(R+R_s)}}{s^\lambda + \frac{1}{C_\lambda(R+R_s)}}, \tag{15}$$

where V_o, V_{in} and $v(0)$ are the output, input and SC initial voltage, respectively. This can be simplified as

$$V_o(s) = \frac{V_{in}(s) + V_{in}(s)\,s^\lambda R_s C_\lambda + v(0)\,s^{\lambda-1}RC_\lambda}{C_\lambda(R+R_s)s^\lambda + 1}. \tag{16}$$

It can be further rearranged and divided by $s^{\lambda-1}$ to both sides of expression yields,

$$V_o(s)C_\lambda(R+R_s)s^1 + V_0(s)s^{1-\lambda} = V_{in}(s)s^{1-\lambda} + V_{in}(s)s^1R_sC_\lambda + v(0)\,RC_\lambda. \tag{17}$$

Since $0 \leqslant \lambda \leqslant 1$, therefore $(1-\lambda) \geqslant 0$, which ensures fractional differentiation and CP derivative is applicable. Taking inverse Laplace of (17), a time domain relation can be obtained as

$$\boldsymbol{\mathcal{D}}^1 v_o(t)C_\lambda(R+R_s) + \boldsymbol{\mathcal{D}}^{1-\lambda}v_o(t) = \boldsymbol{\mathcal{D}}^{1-\lambda}v_{in}(t) + \boldsymbol{\mathcal{D}}^1 v_{in}(t)\,R_sC_\lambda + \delta(t)v(0)\,RC_\lambda, \tag{18}$$

where $\boldsymbol{\mathcal{D}}^{1-\lambda}$ indicates a fractional-order derivative of order $(1-\lambda)$ and $\delta(t)$ depicts a Dirac delta function. According to signal theory and conventional calculus, the first-order derivative of a unit step function is a Dirac delta function, therefore,

$$\boldsymbol{\mathcal{D}}u(t) = \delta(t), \tag{19}$$

where $u(t)$ denotes unit step function. Therefore, expression (18) can be updated as

$$\boldsymbol{\mathcal{D}}^1 v_o(t)C_\lambda(R+R_s) + \boldsymbol{\mathcal{D}}^{1-\lambda}v_o(t) = \boldsymbol{\mathcal{D}}^{1-\lambda}v_{in}(t) + \boldsymbol{\mathcal{D}}^1 v_{in}(t)\,R_sC_\lambda + \boldsymbol{\mathcal{D}}^1 u(t)v(0)\,RC_\lambda. \tag{20}$$

Considering the Haar wavelet features as illustrated in [24], input $v_{in}(t)$, output $v_o(t)$, and unit step function $u(t)$ can be expressed as below.

$$v_o(t) = V_o^T H_M(t), \tag{21}$$

$$v_{in}(t) = V_{in}^T H_M(t), \tag{22}$$

$$u(t) = U^T H_M(t), \tag{23}$$

where $H_M(t)$ is the Haar function vector, M indicates total datapoints, preferably $M = 2^q\,(q = 1, 2, 3..)$, $V_o^T = [v_{o_1}, v_{o_2}, \ldots, v_{o_M}]$ and $V_{in}^T = [v_{in_1}, v_{in_2}, \ldots, v_{in_M}]$ and $U^T = [u_1, u_2, \ldots, u_M]$. Substituting the values of (21)–(23), expression (20) can be rewritten as,

$$V_o^T C_\lambda(R+R_s)\boldsymbol{\mathcal{D}}^1 H_M(t) + V_o^T\boldsymbol{\mathcal{D}}^{1-\lambda}H_M(t) = V_{in}^T\boldsymbol{\mathcal{D}}^{1-\lambda}H_M(t) + V_{in}^T R_sC_\lambda\boldsymbol{\mathcal{D}}^1 H_M(t) + v(0)\,RC_\lambda U^T\boldsymbol{\mathcal{D}}^1 H_M(t) \tag{24}$$

Now, differentiation can be replaced by an operational matrix of derivative as depicted in (10), one can obtain a simple algebraic equation as

$$V_o^T C_\lambda(R+R_s)B^1 H_M(t) + V_o^T B^{1-\lambda}H_M(t) = V_{in}^T B^{1-\lambda}H_M(t) + V_{in}^T R_sC_\lambda B^1 H_M(t) + v(0)\,RC_\lambda U^T B^1 H_M(t). \tag{25}$$

Note that, the complex integral-differential equation of arbitrary fractional-order is transformed into a simple matrix algebra for accurate estimation without much computational complexity. It can be further simplified as

$$V_o^T\left(C_\lambda(R+R_s)B^1+B^{1-\lambda}\right)=V_{in}^TB^{1-\lambda}+V_{in}^TR_sC_\lambda B^1+v(0)\,RC_\lambda U^TB^1.$$

Therefore,

$$V_o^T=\left[V_{in}^T\left(B^{1-\lambda}+R_sC_\lambda B^1\right)+v(0)\,RC_\lambda U^TB^1\right]\left(C_\lambda(R+R_s)B^1+B^{1-\lambda}\right)^{-1}. \tag{27}$$

Finally, using (21), one can obtain time domain output expression as

$$v_o(t)=\left[V_{in}^T\left(B^{1-\lambda}+R_sC_\lambda B^1\right)+v(0)\,RC_\lambda U^TB^1\right]\left(C_\lambda(R+R_s)B^1+B^{1-\lambda}\right)^{-1}H_M(t). \tag{28}$$

This derived equation is sufficient for both charging and discharging data due to the considered initial voltage. Moreover, all the previously reported operational matrix approaches for linear systems were developed with zero initial conditions but, the presented approach is the extended form of the operational matrix approach, with zero and non-zero initial conditions. Hence, expression (28) is the generalized formulation of an R-C series SC impedance model that handles all kinds of the initial state of charge with different charging-discharging profiles. It is to note that this relation can represent the transient characteristics in all charge situations and thus allow to estimate fractional impedance parameters that are independent of the state of charge. Unlike in the previous method, the proposed solution is likely to give a better result for charging and discharging of SC through the same fractional-order equivalent model.

It is always essential to optimize parameter estimation with the minimum error between actual and simulated data. In this work, the non-linear least squares (NLS) data fitting is utilized that allows the identification of parameters for charging and discharging voltage profiles. The NLS is characterized as

$$\min_x||f(x)||_2^2=\min_x\sum_i(f(x)_i)^2, \tag{29}$$

where, $f(x)=v_{data}-v(x)$

where x is the vector of unknown parameters, $v(x)$ is the simulated time-domain output and v_{data} is the real-time output data, whereby the subscript i indicates the ith data point at the sampled time t_i. The constrained NLS problem is solved using the *Trust Region Reflective* (TRR) algorithm, which aims to minimize the NLS problem to substantially zero. We have implemented this routine in MATLAB using the *lsqcurvefit* function to identify the unknown parameter vector x. The algorithm is restricted with positive values for the SC's model to avoid negative results. To note the basic fact that the realization of negative impedance is practically not possible for the supercapacitor, and $-\lambda$ represents the inductor.

5. Experimental study

An experimental setup with SC and measurement DSpace module is depicted in Fig. 2 which was utilized to collect input and output test data. The proposed technique has been validated using real SC data of 1.5 F, 1F and 0.47F values with three different brands: AVX, Kemet, and Eaton as detailed in Table 1. To obtain experimental data, $R=270\ \Omega$, charging voltage $v_{in}=5$ V, and discharging voltage $v_{in}=0$ V, were utilized for all experiments. Collection of data for every input applied and following responses from SCs were recorded for 10 s to 50 s time-frames. In this work, the short transient response is considered that resembles the real-world applications whereby SCs handle the abrupt change in potential. DSpace DS2004ADC module was utilized to collect the data at a sampling rate of 1000 points per second.

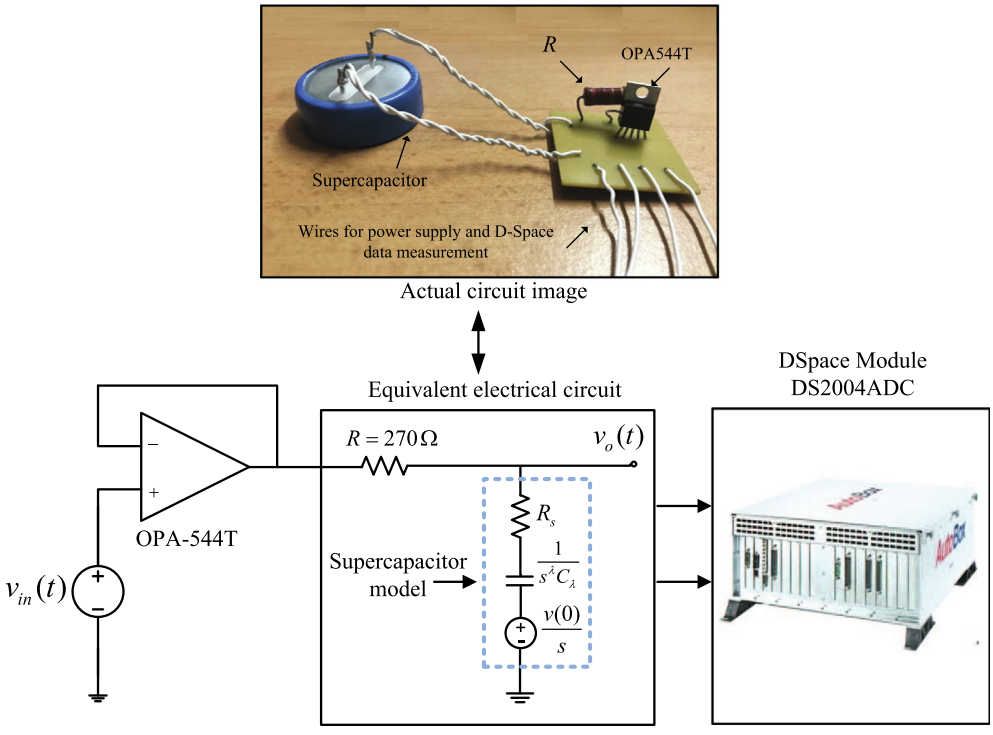

Fig. 2 Experimental setup for supercapacitor with measurement DSpace module.

Table 1 Supercapacitors examined.

Brand	Capacitance	Manufacturer part number
Avx	0.47F	SCMR14F474MRBA0
	1F	SCMR18F105MRBA0
	1.5F	SCMR22F155MRBA0
Kemet	0.47F	FGR0H474ZF
	1F	FR0H105ZF
	1.5F	FE0H155ZF
Eaton	0.47F	KR-5R5C474-R
	1F	KR-5R5V105-R
	1.5F	KR-5R5C155-R

5.1. Analysis with zero initial conditions

Firstly, the impedance parameters have been identified, for fractional and integer-order model considering zero initial conditions, as shown in Table 2. It is to note that the ESR value is very high for both cases.

5.2. Analysis with non-zero initial conditions

The impedance parameters of SC have been estimated for fractional and integer models considering non-zero initial conditions. Table 3 and Table 4 show identified fractional and integer impedance parameters from charging and discharging data respectively with non-zero initial conditions. Furthermore, Fig. 3 (a) shows curve fitting of identified fractional and integer order charging models for Eaton 0.47F and Fig. 3 (b) shows curve fitting of identified fractional and integer order discharging models for Eaton 1.5F. The curve fitting of charging-discharging cycles for AVX 1F is depicted in Fig. 4.

Remark 1. The output voltage Eq. (28) is sufficient for both charging and discharging phase data, unlike the MLF based method [11] wherein two different expressions were derived for charging and discharging phases. Moreover, the proposed method performs calculations without complex programming.

Remark 2. In case of zero initial conditions, the ESR value is very high as shown in Table 2. In contrast to this, the ESR value is very low whenever initial conditions are non-zero and incorporated in modeling equations, as shown in Table 3. According to SC datasheets, ideally, ESR should be very low. Therefore, accurate modeling can be accomplished by considering non-zero initial conditions.

Remark 3. It is clear from Fig. 3 that the fractional models are more accurate than integer-order models to represent and estimate the SC impedance model.

Table 2 Identified model parameters from charging data with zero initial condition.

Supercapacitors		Fractional order model				Integer order model ($\lambda = 1$)		
Brand	Capacitance	$C_\lambda(F/s^{1-\lambda})$	R_s (Ω)	λ	E_t	C_λ (F)	R_s (Ω)	E_t
AVX	0.47F	0.251	187.37	0.871	2.70E−06	0.381	191.21	4.48E−05
	1F	0.419	217.97	0.895	1.33E−06	0.586	219.95	1.03E−05
	1.5F	0.669	189.71	0.907	3.35E−07	0.900	190.84	4.11E−06
Kemet	0.47F	0.041	256.11	0.594	1.33E−04	0.172	295.54	1.20E−03
	1F	0.390	167.84	0.873	1.01E−05	0.587	170.30	2.95E−05
	1.5F	0.542	184.90	0.922	5.21E−07	0.696	186.11	5.16E−06
Eaton	0.47F	0.018	179.26	0.435	1.71E−05	0.152	264.89	4.40E−03
	1F	0.039	257.62	0.413	1.23E−05	0.357	297.33	6.50E−04
	1.5F	0.045	197.16	0.391	2.04E−06	0.456	231.13	7.31E−04

Table 3 Identified model parameters from charging data with non-zero initial condition.

Supercapacitors		Fractional order model				Integer order model ($\lambda = 1$)		
Brand	Capacitance	$C_\lambda(F/s^{1-\lambda})$	R_s (Ω)	λ	E_t	C_λ (F)	R_s (Ω)	E_t
AVX	0.47F	0.476	0.000	0.902	6.18E−06	0.648	1.484	4.48E−05
	1F	0.765	0.000	0.898	1.34E−06	1.060	1.056	1.03E−05
	1.5F	1.147	0.000	0.909	3.37E−07	1.533	0.643	4.11E−06
Kemet	0.47F	0.079	8.918	0.594	1.33E−04	0.325	29.82	1.20E−03
	1F	0.626	2.742	0.873	1.01E−05	0.942	4.273	2.95E−05
	1.5F	0.914	0.069	0.922	5.21E−07	1.172	0.789	5.16E−06
Eaton	0.47F	0.037	0.000	0.471	5.39E−05	0.259	43.15	4.40E−03
	1F	0.081	0.000	0.422	1.26E−05	0.701	19.52	6.50E−04
	1.5F	0.103	0.000	0.443	1.27E−05	0.801	15.49	7.31E−04

Table 4 Identified model parameters from discharging data with non-zero initial condition.

Supercapacitors		Fractional order model				Integer order model ($\lambda = 1$)		
Brand	Capacitance	$C_\lambda(F/s^{1-\lambda})$	R_s (Ω)	λ	E_t	C_λ (F)	R_s (Ω)	E_t
AVX	0.47F	0.457	0.000	0.933	2.60E−06	0.562	1.125	1.85E−05
	1F	0.744	0.000	0.935	1.32E−06	0.914	0.733	5.60E−06
	1.5F	1.056	0.000	0.935	3.77E−07	1.295	0.514	2.16E−06
Kemet	0.47F	0.092	7.911	0.619	1.34E−04	0.344	25.70	1.14E−03
	1F	0.507	3.481	0.839	9.11E−06	0.855	5.713	2.76E−05
	1.5F	0.804	0.156	0.927	3.81E−07	1.014	0.929	3.59E−06
Eaton	0.47F	0.038	0.000	0.473	5.98E−05	0.259	42.75	4.49E−03
	1F	0.095	0.205	0.448	1.50E−05	0.727	17.09	6.45E−04
	1.5F	0.093	0.000	0.439	1.71E−05	0.737	17.10	7.31E−04

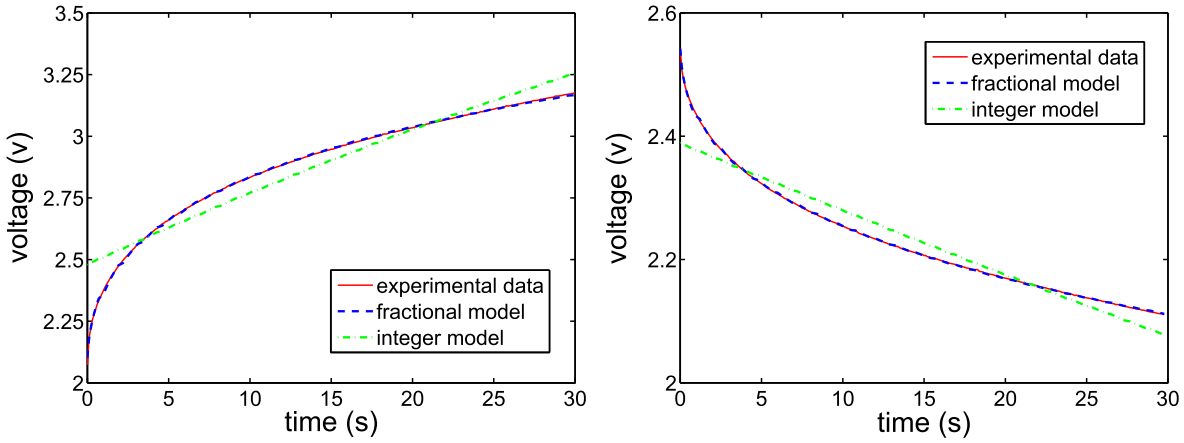

Fig. 3 Identified supercapacitor models with non-zero initial conditions: (a) Eaton 0.47F charging model (b) Eaton 1.5F discharging model.

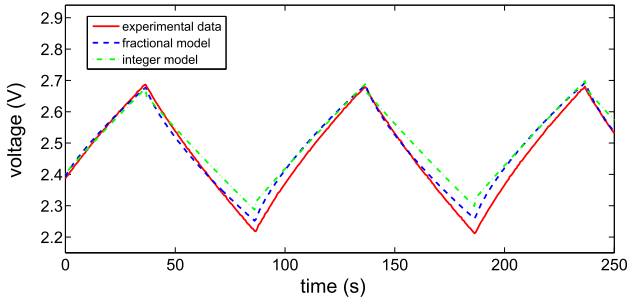

Fig. 4 RC models with long data of charging-discharging cycles: AVX 1F.

5.3. Analysis for different time-frame data with zero and non-zero initial conditions

Further investigation is presented in Table 5, with only charging model parameters. The result is obtained from SC AVX 1.5F with zero and non-zero initial voltages and different time-frame data. When initial voltage is considered, there is a very small variation in parameter values. However, that is not because of initial voltage dependency, but due to the chemical properties of a material, external environmental condition, and other internal phenomena of SCs. Furthermore, the identified parameters in Table 5 reflect that the internal series resistance (R_s) is very small, which is justified as per value in datasheet by manufacturers.

Moreover, when we used AVX 1.5F charging model (with non-zero initial conditions as shown in Table 3) to curve fit with other data of different initial state of charges and time-frames, it shows good accuracy for different datasets with the same parametric model, as shown in Fig. 5 (a). Similarly, for Kemet 1.5F discharging model, again it shows good agreement. However, in case of zero initial conditions for AVX 1.5F charging model (as shown in Table 2), the same parametric model is not sufficient to represent different datasets. It is clearly depicted in Fig. 6. Hence, the model parameters are necessary to update for different datasets, even for the same SC value and that was the demerit from previously reported approaches.

Remark 4. The standard parametric model can be estimated using the proposed scheme with non-zero initial conditions for any SC with acceptable slight variation in parameter values,

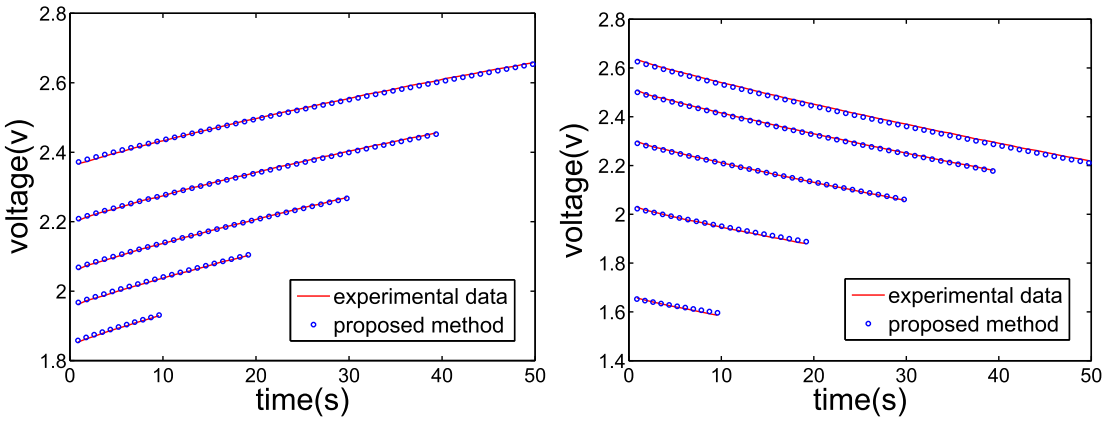

Fig. 5 Supercapacitor models (non-zero initial condition) with different initial voltages and time duration: (a) AVX 1.5F charging model (b) Kemet 1.5F discharging model.

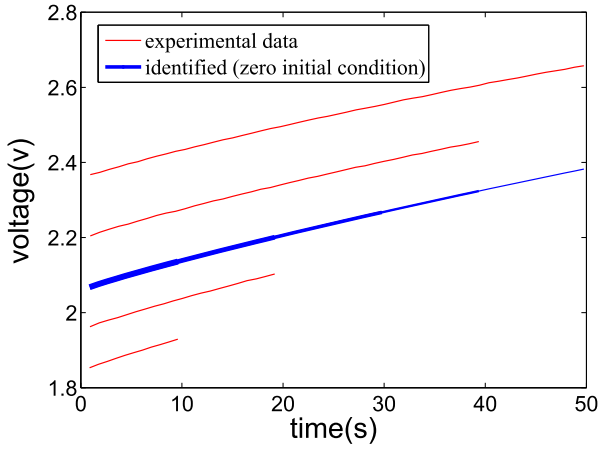

Fig. 6 Same model performance with initial voltages and time span: AVX 1.5F.

irrespective of charging, discharging, different initial condition, and time-frame of experimental data.

5.4. Comparison with existing methods

One more investigation was carried out with the charging model parameters obtained from the supercapacitor AVX 1F as in Table 3. Fig. 7 (a) and (b) depict the accurate curve fitting with the real data, though different initial state of charges and

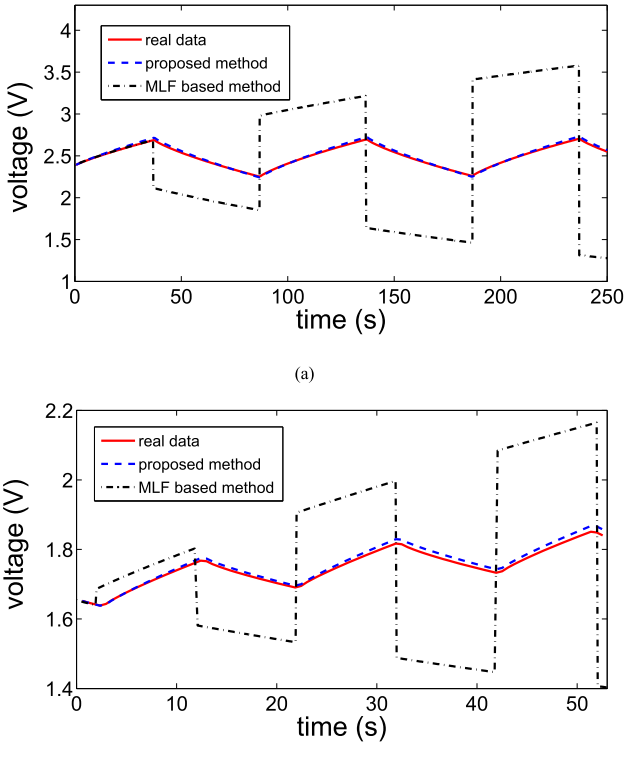

Fig. 7 Comparison with MLF method [20] for charging-discharging cycles: AVX 1F supercapacitor.

Table 5 Identified model parameters from charging data (zero/non-zero initial conditions and different time-frame).

Supercapacitor	Time-frame	zero initial conditions				non-zero initial conditions			
AVX 1.5 (F)	T (sec)	$C_\lambda(F/s^{1-\lambda})$	$R_s(\Omega)$	λ	E_t	$C_\lambda(F/s^{1-\lambda})$	$R_s(\Omega)$	λ	E_t
	10	0.771	158.93	0.922	2.92E−07	1.275	0.00	0.939	3.17E−07
	20	0.737	174.44	0.918	3.05E−07	1.219	0.00	0.919	3.06E−07
	30	0.669	189.71	0.907	3.35E−07	1.147	0.00	0.909	3.37E−07
	40	0.603	212.74	0.894	3.81E−07	1.101	0.00	0.899	4.10E−07
	50	0.541	242.01	0.885	5.40E−07	1.138	0.00	0.911	1.42E−06

time span, using the same estimated model parameters. For fair comparison MLF method with non-zero initial conditions [20] was considered in Fig. 7. For the first charging phase, the MLF method and the proposed method show similar accuracy. However, the MLF method could not follow real data after the first charging phase due to its time dependency. It clearly indicates that the proposed method is accurate and able to extract standard parametric model independent of time span and initial voltages. Unlike MLF based methods, with zero initial conditions [11] and with non-zero initial conditions [15], the proposed method works closely with real-time varying charging-discharging values.

6. Conclusions

In this paper, the primary objective is kept to estimate the SC's fractional impedance without direct measurement from the impedance analyzer. Generally, such equipment is very costly, therefore, the proposed technique helps to measure the fractional impedance from simple test data. The presented idea facilitates to identify the SC fractional impedance model accurately without adding computational complexity of fractional derivatives. An operational matrix approach has been opted using the Haar wavelet that resulted the more generalized output expression to represent the charging and discharging profiles. More importantly, it has been shown from results that the estimated parameter values can fit with any initial voltage and timeframe data. The experimental study has proven the merits of the presented scheme. In future, considering non-zero initial conditions, the study could be extended for other complex models instead of the RC series model.

Declaration of Competing Interest

The authors declare that they have no known competing financial interests or personal relationships that could have appeared to influence the work reported in this paper.

References

[1] J. Libich, J. Máca, J. Vondrák, O. Cech, M. Sedlaríková, Supercapacitors: Properties and applications, J. Energy Storage 17 (2018) 224–227.

[2] A. Allagui, T.J. Freeborn, A.S. Elwakil, M.E. Fouda, B.J. Maundy, A.G. Radwan, Z. Said, M.A. Abdelkareem, Review of fractional-order electrical characterization of supercapacitors, J. Power Sources 400 (2018) 457–467.

[3] M. Kumar, S. Ghosh, S. Das, Analytical formulation for power, energy, and efficiency measurement of ultracapacitor using fractional calculus, IEEE Trans. Instrum. Meas. 68 (12) (2019) 4834–4844.

[4] A. Eddahech, M. Ayadi, O. Briat, J.-M. Vinassa, Online parameter identification for real-time supercapacitor performance estimation in automotive applications, Int. J. Electr. Power Energy Syst. 51 (2013) 162–167.

[5] G. Sun, Y. Liu, R. Chai, F. Mei, Y. Zhang, Online model parameter identification for supercapacitor based on weighting bat algorithm, AEU Int. J. Electron. Commun. 87 (2018) 113–118.

[6] L. Helseth, Modelling supercapacitors using a dynamic equivalent circuit with a distribution of relaxation times, J. Energy Storage 25 (2019) 100912.

[7] C.A. Monje, Y. Chen, B.M. Vinagre, D. Xue, V. Feliu-Batlle, Fractional-order Systems and Controls, Springer-Verlag, London, 2010.

[8] K. Kothari, U. Mehta, R. Prasad, Fractional-order system modeling and its applications, J. Eng. Sci. Technol. Rev. 12 (6) (2019) 1–10.

[9] V. Gill, K. Modi, Y. Singh, Analytic solutions of fractional differential equation associated with RLC electrical circuit, J. Stat. Manage. Syst. 21 (4) (2018) 575–582.

[10] R. Prasad, U. Mehta, K. Kothari, Various analytical models for supercapacitors: a mathematical study, Resource-Efficient Technol. 1 (2020) 1–15.

[11] T.J. Freeborn, B. Maundy, A.S. Elwakil, Measurement of supercapacitor fractional-order model parameters from voltage-excited step response, IEEE J. Emerg. Sel. Top. Circ. Syst. 3 (3) (2013) 367–376.

[12] T.J. Freeborn, Estimating supercapacitor performance for embedded applications using fractional-order models, Electron. Lett. 52 (17) (2016) 1478–1480.

[13] T.J. Freeborn, A.S. Elwakil, Rates and effects of local minima on fractional-order circuit model parameters extracted from supercapacitor discharging using least squares optimization, Circ. Syst. Signal Process. 38 (2019) 1907–1922.

[14] V. Martynyuk, M. Ortigueira, Fractional model of an electrochemical capacitor, Signal Process. 107 (2015) 355–360.

[15] R. Prasad, K. Kothari, U. Mehta, Flexible fractional supercapacitor model analyzed in time domain, IEEE Access 7 (2019) 122626–122633.

[16] L. Zhang, X. Hu, Z. Wang, F. Sun, D.G. Dorrell, Fractional-order modeling and state-of-charge estimation for ultracapacitors, J. Power Sources 314 (2016) 28–34.

[17] K.A. Abro, P.H. Shaikh, J. Gomez-Aguilar, I. Khan, Analysis of De-Levie's model via modern fractional differentiations: An application to supercapacitor, Alexandria Eng. J. 58 (4) (2019) 1375–1384.

[18] Z. Bououchma, J. Sabor, H. Aitbouh, New electrical model of supercapacitors for electric hybrid vehicle applications, Mater. Today: Proc. 13 (2019) 688–697.

[19] J.M. Baptista, J.S. Sagu, U. Wijayantha, K. Lobato, State-of-the-art materials for high power and high energy supercapacitors: Performance metrics and obstacles for the transition from lab to industrial scale - a critical approach, Chem. Eng. J. 374 (2019) 1153–1179.

[20] R. Prasad, U. Mehta, K. Kothari, M. Cirrincione, A. Mohammadi, Supercapacitor parameter identification using grey wolf optimization and its comparison to conventional trust region reflection optimization, in: 2019 International Aegean Conference on Electrical Machines and Power Electronics (ACEMP) & 2019 International Conference on Optimization of Electrical and Electronic Equipment (OPTIM), 2019, pp. 563–569.

[21] AVX Corporation, SCM Series-Connected Supercapacitor Modules.

[22] M.D. Ortigueira, F.J.V. Coito, On the usefulness of Riemann-Liouville and Caputo derivatives in describing fractional shift-invariant linear systems, J. Appl. Nonlinear Dyn. 1 (2) (2012) 113–124.

[23] I. Podlubny, Fractional Differential Equations: An Introduction to Fractional Derivatives, Fractional Differential Equations, to Methods of Their Solution and Some of Their Applications, Mathematics in Science and Engineering, Elsevier Science, 1998.

[24] K. Kothari, U. Mehta, J. Vanualailai, A novel approach of fractional-order time delay system modeling based on Haar wavelet, ISA Trans. 80 (2018) 371–380.

[25] Y. Li, X. Meng, B. Zheng, Y. Ding, Parameter identification of fractional order linear system based on Haar wavelet operational matrix, ISA Trans. 59 (2015) 79–84.